Available online at www.sciencedirect.com

SCIENCE DIRECT®

Earth and Planetary Science Letters 219 (2004) 255–269

EPSL

www.elsevier.com/locate/epsl

Large-scale geometry, offset and kinematic evolution of the Karakorum fault, Tibet

Robin Lacassin[a,*], Franck Valli[a], Nicolas Arnaud[b], P. Hervé Leloup[c], Jean Louis Paquette[d], Li Haibing[a,e], Paul Tapponnier[a], Marie-Luce Chevalier[a], Stephane Guillot[c], Gweltaz Maheo[c], Xu Zhiqin[e]

[a] Laboratoire de Tectonique, Mécanique de la Lithosphère, UMR 7578 CNRS, Institut de Physique du Globe de Paris, 75252 Paris CX05, France

[b] Laboratoire de Dynamique de la Lithosphère, UMR 5573 CNRS, ISTEEM - USTL, Place Eugène Bataillon, 34095 Montpellier CX5, France

[c] Laboratoire de Dynamique de la Lithosphère, UMR 5570 CNRS, UCB Lyon et ENS Lyon, 2 rue Dubois, 69622 Villeurbanne, France

[d] Laboratoire Magmas et Volcans, UMR 6524 CNRS, Université Blaise Pascal, Rue Kessler, 63038 Clermont Ferrand CX, France

[e] Institute of Geology, Chinese Academy of Geological Sciences, 26 Baiwanzhuang Road, Beijing 100037, PR China

Received 16 September 2003; received in revised form 18 December 2003; accepted 18 December 2003

Abstract

The total offset, lifespan and slip rate of the Karakorum fault zone (KFZ) (western Tibet) are debated. Along the southern fault half, ongoing oblique slip has exhumed dextrally sheared gneisses intruded by synkinematic leucogranites, whose age ($\sim$23 Ma, U/Pb on zircon) indicates that right-lateral motion was already in progress in the late Oligocene. Ar/Ar K-feldspar thermochronology confirms that rapid cooling started around 12 Ma, likely at the onset of the present dextral normal slip regime. Correlation of suture zones across the fault requires a total offset greater than 250 km along the active – northern – fault branch. An average long-term slip rate of 1 ± 0.3 cm/yr is inferred assuming that this offset accrued in a time span of 23–34 Ma. Southwest of the Ladakh-Karakorum Range, the large-scale boudinage of ophiolitic units suggests that an offset of several hundreds of kilometers exists along another – southern – branch of the KFZ. Towards the southeast, in the Mount Kailas region, the fault zone does not end at Gurla Mandatha, but continues eastwards, as a transpressive flower structure, along the Indus–Tsangpo suture. Our new data thus suggest that the KFZ contributed to absorb hundreds of kilometers of India–Asia convergence.

Keywords: tectonics; geochronology; shear zone; strike-slip fault; collision; Asia; Tibet

1. Introduction

Discriminating between localized and distributed deformation in the continental lithosphere requires precise knowledge of time-dependent slip rates and offsets along faults. In northern

* Corresponding author. Tel.: +33-1 44 27 26 01 or +33-1 44 27 39 05; Fax: +33-1 44 27 24 40.
E-mail address: lacassin@ipgp.jussieu.fr (R. Lacassin).

0012-821X/04/$ – see front matter © 2004 Elsevier B.V. All rights reserved.
doi:10.1016/S0012-821X(04)00006-8

and eastern Tibet, there is convincing evidence that only a few large fault zones contributed to absorb and transfer eastwards a large fraction of the convergence between India and Asia. In Yunnan and Sichuan, for instance, the Ailao Shan–Red River shear zone, acting as a lithospheric plate boundary between South China and Indochina, accrued 700 ± 200 km of sinistral offset in a minimum time span of 16 Myr, at an average rate of ~ 4 cm/yr (e.g. [1,2]). Along the edge of the Tarim, the Altyn Tagh fault also appears to cut the lithosphere (e.g. [3]) and contributed to move Tibet ~ 500 km eastwards since collision began [4–7]. By contrast, deformation along the southern boundary of the plateau, north of the Himalayas, is poorly understood, and the NW–SE-trending, dextral Karakorum fault (KF) is the least studied and presently most controversial of Asia's large Tertiary geological discontinuities.

For about 1000 km, it follows the SW edge of Tibet (Fig. 1). Its contemporary and late Pleistocene slip rates are in dispute (≈ 3 cm/yr [4,8,9]; ≈ 4 mm/yr [10,11]). Few markers unambiguously constraining pre-Pliocene movement have been described and dated. Some have been taken to

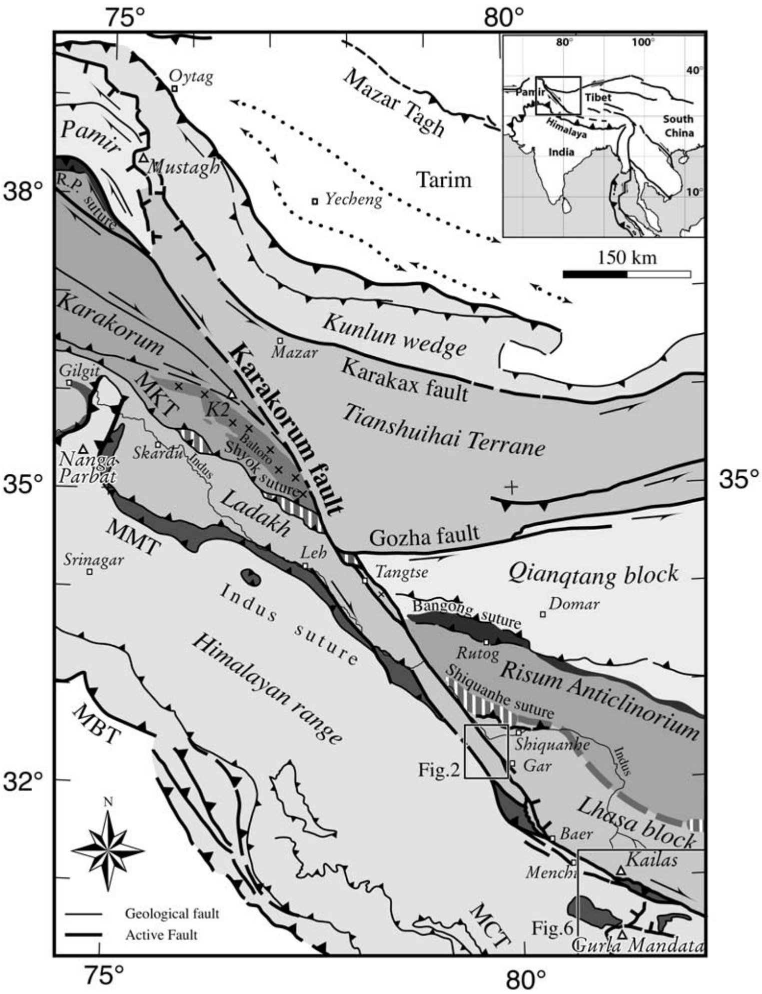

Fig. 1. Large-scale sketch map of KFZ and adjacent units. Inset shows location in large-scale Asian tectonic framework. Dark-gray tones outline the Indus-Zangbo, and the Bangong-Nujiang/Rushan-Pshart (R.P.) suture zones. Hatched tones correspond to Shiquanhe and Shyok suture zones.

imply dextral shear since 11 Ma [4], less than 17 Ma [12] or 13 Ma [11,13]. Estimates of possible offsets range over one order of magnitude ($\sim$1000 km [14]; $>$115 km [8,15]; $\sim$200 km [16]; $\approx$300 km [4]; 85, 90, 120, 150 km [12,17]; 66 km [11,13]). Interpretations concerning the large-scale geometry, evolution and role of the fault also differ widely. Some authors infer that, due to partitioning of oblique convergence between India and the extruding Tibet plateau [18], it has taken up large amounts of cumulative dextral motion, with former strands continuing eastward along the Zangbo suture and the Jiali fault [14,19,20]. In contrast, Murphy et al. [11,13] contend that it does not extend past Kailas, with the Gurla Mandatha detachment absorbing all the dextral slip left at its southern tip.

From detailed mapping and dating of sheared rocks along the southern fault half (Fig. 1), we present here new evidence that helps assess the kinematic evolution of the fault, and supports quantitatively the former scenario.

2. Structural and kinematic constraints from the Karakorum Range mylonites

Southwest of Shiquanhe ($\sim$32.5°N, Fig. 1), the active KF splays into oblique strands that offset Quaternary fans and moraines, most prominently along the western edge of the Gar pull-apart basin (Figs. 1 and 2) [8,20]. The normal throw has been large enough to exhume metamorphic and magmatic footwall rocks, which form the SE termination of the Ladakh-Karakorum Range (Fig. 1). For at least 30 km along strike, mylonites and gneisses with unambiguous evidence of strong ductile shear are well exposed on uplifted triangular facets and in hanging glacial valleys [4]. We mapped and sampled these rocks along six sections, which display structures similar to that shown on Fig. 3. The shear zone is at least $\sim$500 m wide, with N135°E-trending, 40–70°NE-dipping foliation, horizontal stretching lineation and dextral, mostly C/S, shear indicators (Figs. 3 and 4a,b). The metamorphic grade increases southwestwards from the range front. A greenschist mylonite zone up to 10 m thick follows this front, with brittle-ductile deformation (oblique lineations and meter-scale shear bands, Fig. 3) consistent with oblique normal slip, as along the adjacent active fault. Away from the range front, leucocratic melt veins sheared to various degrees become inter-layered with the gneiss mylonites (Fig. 4c). Foliation in the most strongly sheared veins is parallel to the surrounding gneiss foliation (Fig. 4d). Several generations of veins are often observed on a same outcrop, with late, weakly deformed veins cutting strongly sheared ones (Fig. 4c). Although some migmatization is observed in situ, the main source rock of such veins is probably located farther SW, where pervasive melt invades the footwall (Fig. 3). Though less strong, the strike-slip shear imprint remains clear in the larger leucocratic intrusions (e.g. Fig. 4a) and migmatites that form the core of the range. Such field relationships imply anatexy and intrusion coeval with dextral shearing.

3. Ages of crystallization and cooling of mylonites and sheared anatectic granites

Results of U/Pb and $^{40}Ar/^{39}Ar$ dating, which will be discussed in detail in a forthcoming paper, imply that the deformed leucogranites are of Oligocene age and have been exhumed in the mid-Miocene. Conventional U/Pb thermo-ionization dating on zircons yields concordant ages at 22.7 ± 0.1 Ma (Fig. 5a). Some discordant zircon ages are consistent with a poorly defined lower intercept at 32 ± 3 Ma, and a Proterozoic (1300 ± 100 Ma) upper intercept (Fig. 5a). High-resolution in situ dating (CAMECA IMS 1270 ion microprobe, CRPG-CNRS, Nancy) of 17 zircons (24 spots) from different samples confirms these results. Four zircons from the K1P20 mylonite yield comparable, concordant ages ranging between 20 and 25 Ma in their cores and rims (Fig. 5a). Inherited zircon ages range from Paleozoic to Precambrian ($\sim$1200 Ma). Some of them appear to have recrystallized partially during Tertiary deformation, yielding discordant ages, the youngest being 34 ± 0.8 Ma. The cooling history of the mylonites is well constrained by $^{40}Ar/^{39}Ar$ dating on biotite and K-feldspars from seven different sam-

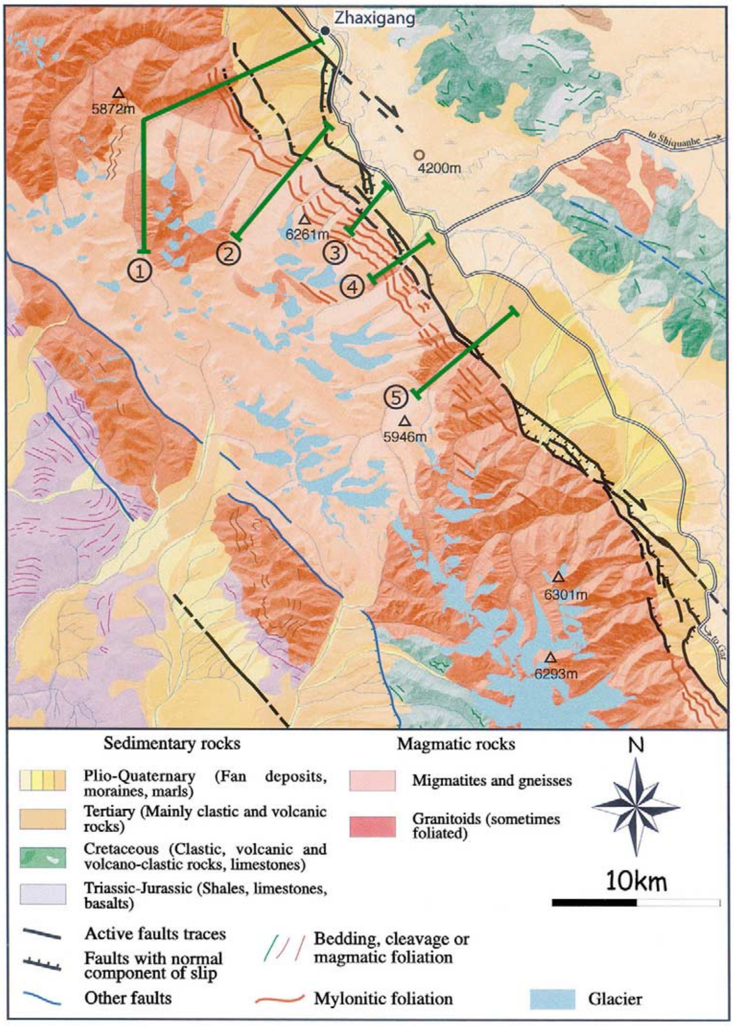

Fig. 2. Geological map of Ladakh-Karakorum Range between Zhashikang and Gar, west of Shiquanhe. Drawn from field observations and satellite (Landsat, Spot) image interpretation. Light shading outlines topography. Five sections studied in the field are shown by green lines. Section 6 is located ~40 km south, near Gar city.

ples (Fig. 5b). Modeling of K-feldspar age spectra [21] suggests slow cooling (14°C/Ma) starting at ≈25 Ma followed by a phase of very rapid cooling (150°C/Ma) that took place at ~12 Ma in section 1 and 8 Ma in the other sections (Fig. 5b). One biotite gave a well-defined plateau age, around 14 Ma, compatible with the K-feldspar cooling history, while one apatite fission track age at 9 Ma [22] is consistent with the ~8 Ma rapid cooling deduced from K-feldspar modeling (Fig. 5b).

4. Continuation of the fault east of 81°E

South of Baer (Fig. 1), ductile sheared rocks have not yet been found in situ, but the evidence for Neogene and recent strike-slip faulting is remarkably clear. In the field and on SPOT, LANDSAT (Fig. 6a) and ASTER images, we mapped several parallel active fault strands that offset fluvial fans and glacial moraines between Hor and Mens (Fig. 6b). At about 80.5°E, the trend of the fault zone swings rapidly from

≈N135 to ≈N105°E (Fig. 1). On occasion of this ≈30° bend, most of the active strands east of Menshi come to hug the Kailas (Fig. 6b) rather than the Ladakh range front as they do north of Baer (Fig. 2). Concurrently, the spectacular transtension observed all along the Gar–Baer pull-apart gives way to more subdued transpression and folding. There is no visible branch of the KF along the southern edge of the Barga-Menshi trough, which appears to be a piggy-back sag comparable to the greater Sutlej basin [23] to the west. Neither is there any evidence that the Amlang La ophiolite klippe [23] is cut by faults with significant dextral slip (Fig. 6b,c). Therefore, the postulated extension of the Karakorum fault zone (KFZ) inferred by Murphy et al. [11] to meet with the Gurla-Mandatha detachment southwest of Lake Raksas does not appear to exist. On the other hand, one splay of the KFZ veers into the active normal faults that bound the east side of Lake Manasarovar (Fig. 6b) whose formation, unlike that of Lake Raksas, thus clearly results from Quaternary extension. These faults are connected, through a ≈20-km-long en echelon array of oblique, right-stepping faults that acts as a sinistral transfer zone, with the active, left-stepping normal faults that follow the east side of the Pulan half graben (Fig. 6b). Together, these faults form a small N–S Quaternary rift comparable to those found eastwards in southern Tibet [16,24]. Since the Amlang La and Lalung Ri ophiolite klippes (west and east of Manasarovar, Fig. 6c) lie at the same structural level, the total throw on all these steeply west-dipping normal faults is unlikely to exceed a few kilometers (≤10 km), again as in most of the south Tibetan rifts [24].

As is typical of the relationship between rifts and dextral faults in southern Tibet [20], active branches of the KFZ clearly continue eastwards, past the Manasarovar-Pulan half graben, to Lake Kunggyu (82.5°E, Fig. 6b), and farther. Near Darchen and north of Barga (Fig. 6b), the oblique dextral strands of the KFZ that cut the Quaternary piedmont bajada merge with the Kailas-Ponri Range front faults and penetrate into the range (Fig. 6b). We interpret the active southward

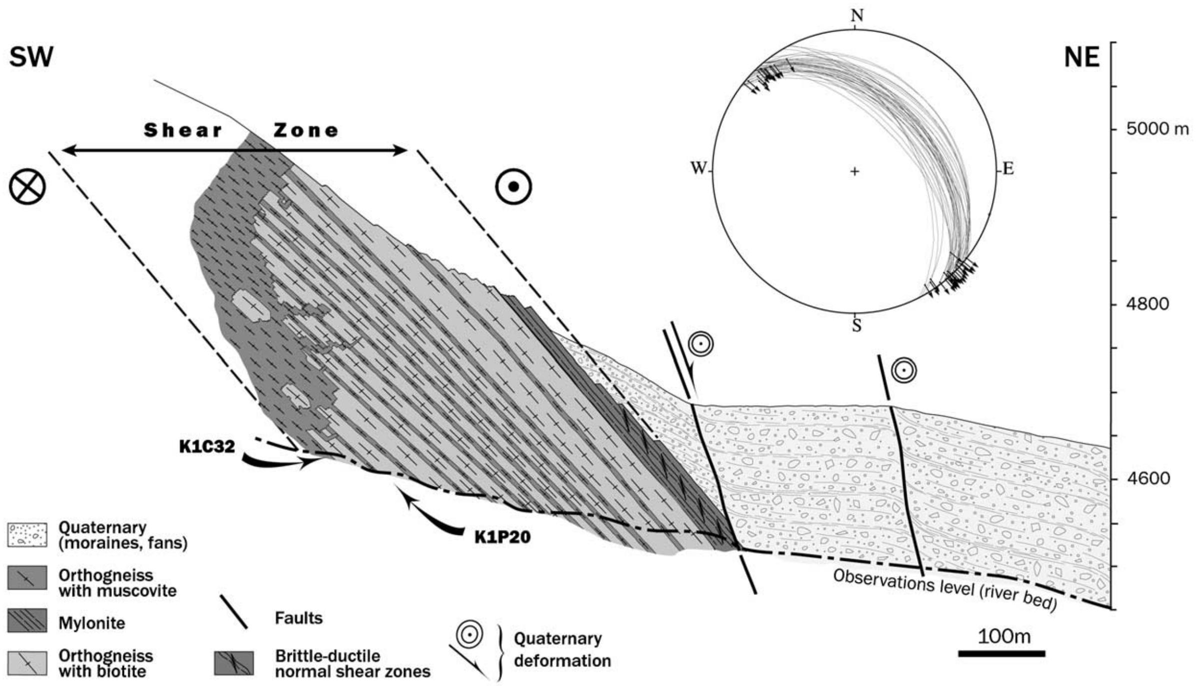

Fig. 3. Typical section of mylonites and gneisses west of Shiquanhe (section 4, Fig. 2); Schmid diagram (lower hemisphere) shows geometry of foliations (great circles) and of lineations (arrows). Samples dated with U/Pb techniques (Fig. 5) are located.

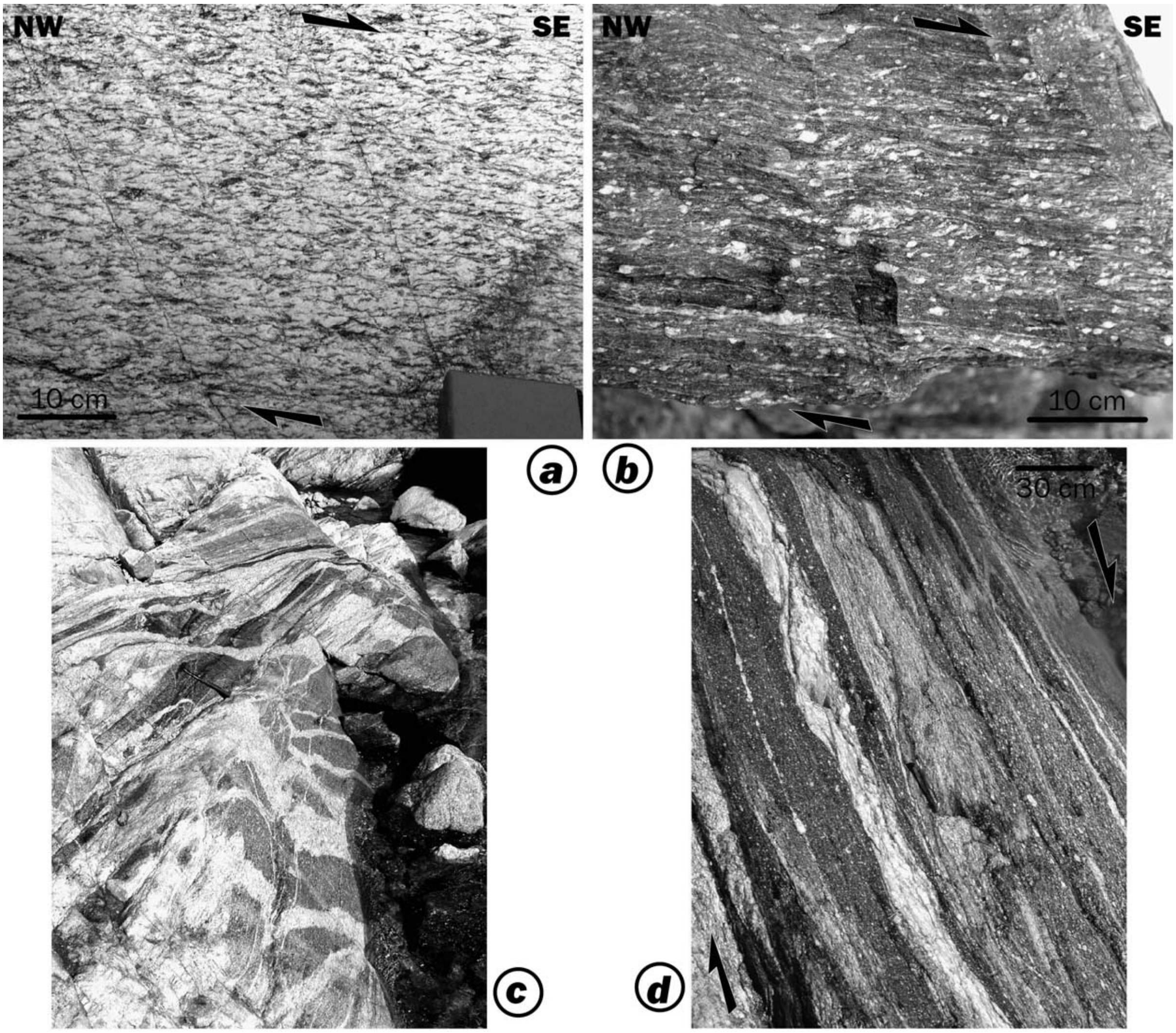

Fig. 4. Characters of deformation in gneisses and mylonites. a: C/S leucogranitic gneiss (section 4, Fig. 2). b: Dextrally sheared mylonites close to range front (section 3, Fig. 2). c: Several generations of synkinematic leucocratic veins intruding biotite-bearing gneisses (section 4, Fig. 2). d: Example of dextrally sheared leucocratic vein and gneisses (section 4, Fig. 2).

thrust component of motion on these faults, which is clear from folding of late Cenozoic markers, to be responsible for the Neogene uplift of the Kailas and the local incision of the > 2000-m-thick Tertiary molasses it is built of (Fig. 7a). The southern part of the range (Figs. 6c and 7a; southern Kailas flysch and mélange of Gansser [23]) is made of steep, meter to kilometer size fault-bounded slivers including brecciated, steeply schistosed serpentinites, cherts, sandstones and pelites (Fig. 6d). Within the slivers and on their bounding faults, there is clear evidence (horizontal slickensides, C/S indicators, asymmetric boudinage, Fig. 7b,c) for brittle dextral shear, combined with folds and reverse faults. On a larger scale, our mapping implies that the long documented folds and thrusts, some of which north-vergent [23,25], are connected to the KFZ strike-slip strands (Fig. 6b,c). Thus, both the outcrop-scale deformation and the regional geometry concur to show that the main KFZ continues east of 81°E as a dextral, transpressive flower structure

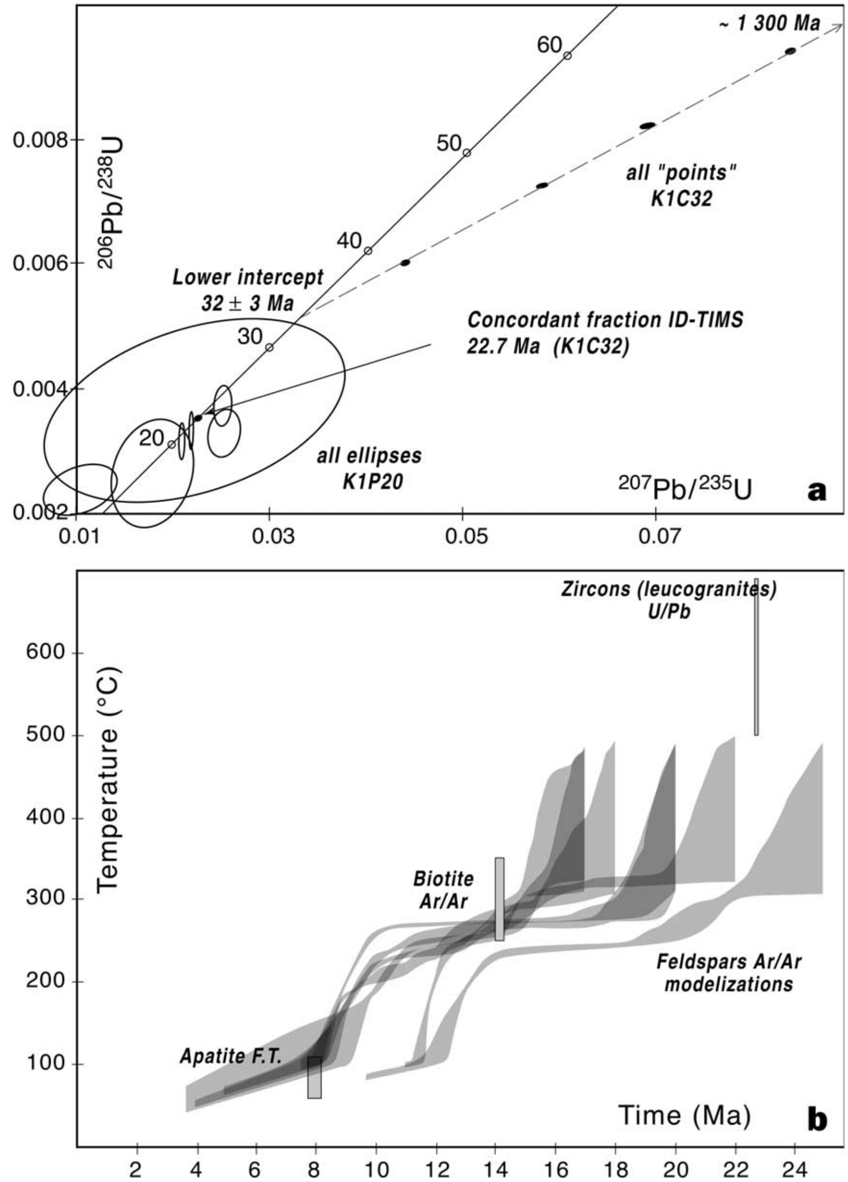

Fig. 5. Age results on gneisses and mylonites from sections 1–5 (Fig. 2). a: Concordia diagram showing U/Pb results on leucogranites from section 4 (Fig. 3). Small black ellipses show results obtained on different zircon fractions from sample K1C32 (2σ error); large open ellipses show concordant zircon ages from microprobe dating (sample K1P20); both samples are located on Fig. 3. b: Summary of cooling histories deduced from Ar/Ar dating; grayed areas: results of K-feldspar modeling [21] within 2σ error (seven samples coming from sections 1–5). Results obtained for one biotite, U/Pb zircon age of leucogranites (this study), and one apatite fission track age [22] are also shown for comparison.

reactivating the Indus-Tsangpo suture (Fig. 6d). This interpretation accounts well for two of the Gansser's fundamental observations [23]: the juxtaposition in map view, due to large lateral offsets, of slices of widely different rock types yielding a strike-slip tectonic 'mélange'; and the existence of the well-known, north-directed south Kailas thrust, which bounds a large lens of suture

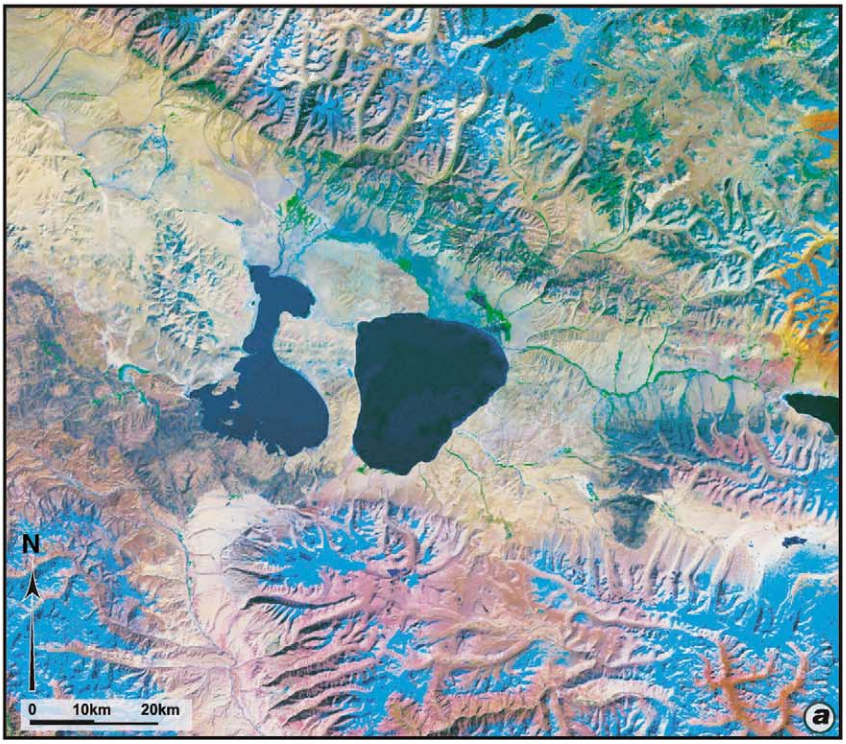
N
0
10km
20km
a

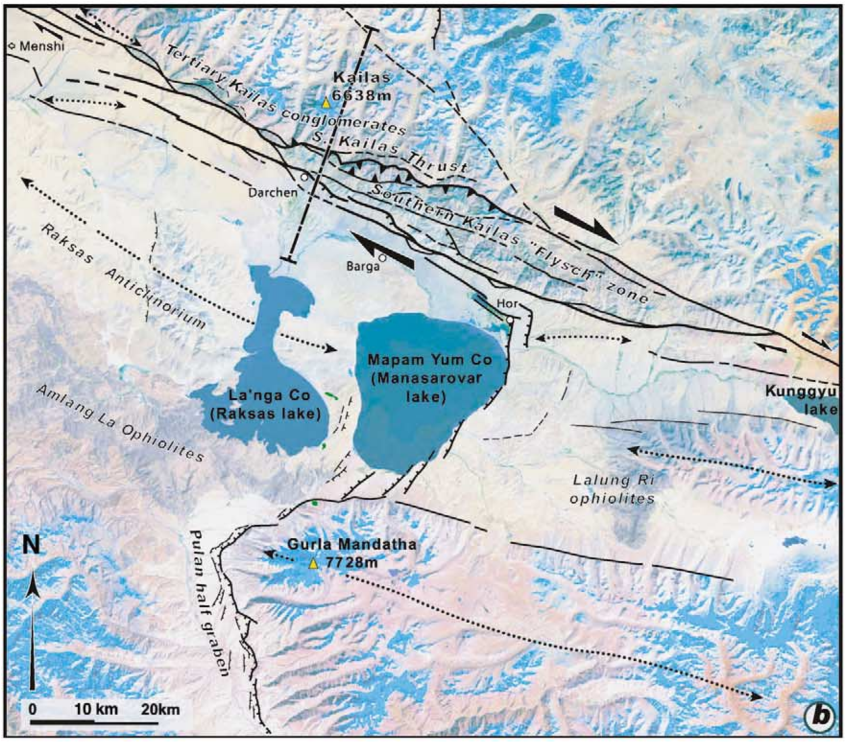
Menshi
Tertiary Kailas conglomerates
Kailas
6638m
S. Kailas Thrust
Darchen
Southern Kailas "Flysch" zone
Barga
Raksas Anticlinorium
Hor
Mapam Yum Co
(Manasarovar
lake)
La'nga Co
(Raksas lake)
Amlang La Ophiolites
Kunggyu
lake
Lalung Ri
ophiolites
Gurla Mandatha
7728m
Pulan half graben
N
0
10 km
20km
b

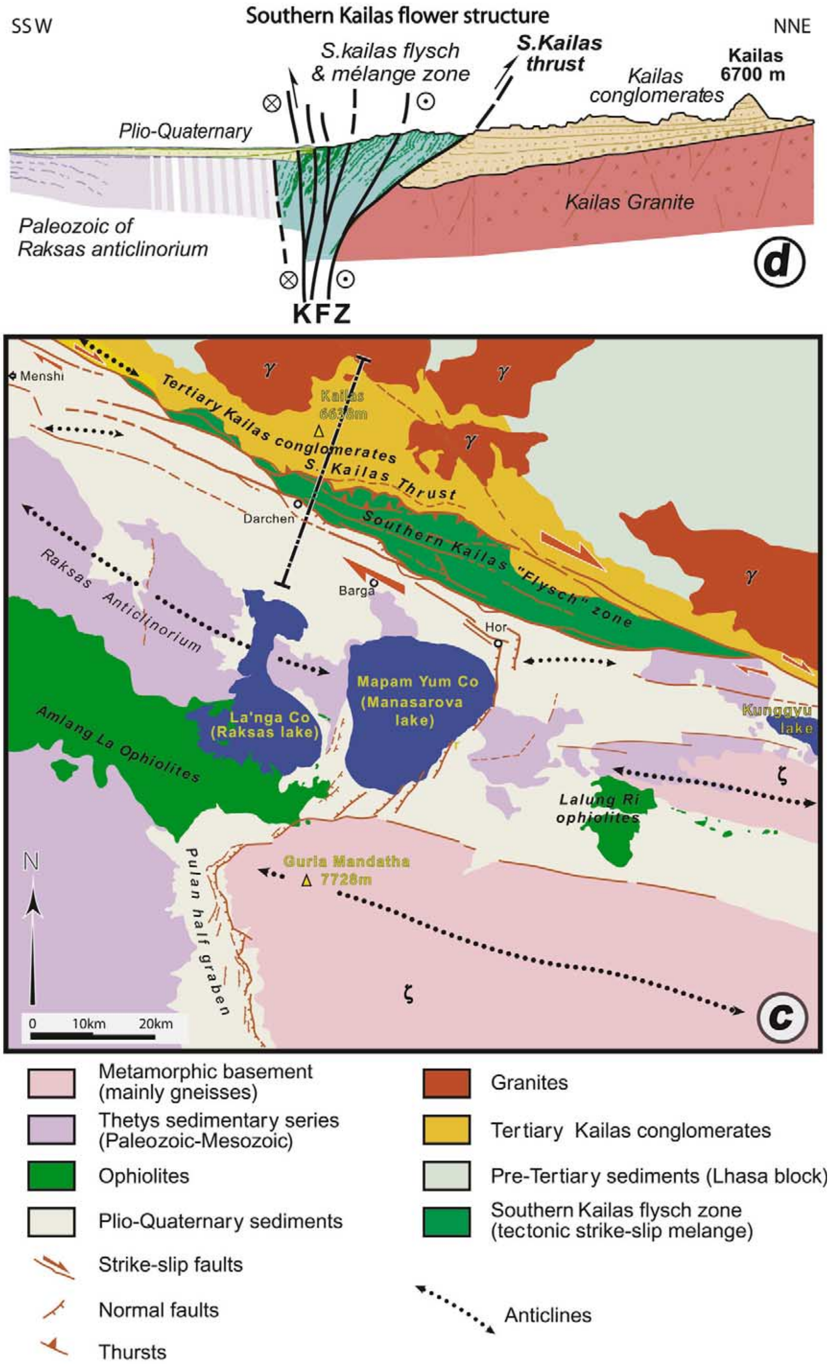

Fig. 6. Geometry of southern KFZ in Kailas region. a: Part of Landsat 7 image. b: Fault trace geometry, after field observations, geological maps [11,23,34] and satellite image interpretation, on Landsat image. c: Corresponding structural sketch. d: Interpretation of Gansser [23] synthetic section of the Kailas Range; approximative location of section shown by black hatched line on structural sketch.

rocks, forming locally the northern edge of the flower (Fig. 6c,d).

5. Discussion: timing, offset and length of the KFZ

Our new structural and age data between Zhaxigang and Hor suggest that recent interpretations that downplay the total offset, length, age and role of the KFZ should be revised.

The ductile mylonites along the northwest boundary of the Gar pull-apart [4] formed as a result of dextral shear at least as early as 23 Ma ago, and possibly earlier (>34 Ma), taking into account K1C32 lower intercept age (Fig. 5). As along the Ailao Shan–Red River shear zone [1,2], such shear lasted for millions of years and possibly caused partial melting, resulting in synkinematic leucogranite emplacement. Clearly, the lifespan of the KFZ as a dextral crustal-scale fault has been longer than hitherto inferred [4,11–13]. It must have started at the end of the Oligocene (≈ 25 Ma), or possibly of the Eocene (≈ 35 Ma). This suggests that the sheared Tangtse (Fig. 1) granite, whose age (17 Ma) was taken by Searle et al. [12] to provide a lower bound for the onset of right-lateral slip, could have formed as a result of melting during shear, like the leucogranites we date here near Zhaxikang, or have dated along the Ailao Shan–Red River zone [26]. Note that Weinberg and Searle [27] also mentioned this alternative interpretation. As pointed out by Leloup et al. [1], such deformed leucogranites should not be used as offset markers along strike-slip fault zones.

The cooling history recorded by the rocks near Zhaxigang indicates that a marked kinematic change from purely dextral to dextral normal motion occurred around or just after 12 Ma. Such oblique motion, which continues today, likely formed and exhumed the greenschist mylonites found at the very edge of the Ladakh Range. It also resulted in the development and deepening of the Gar and Baer pull-apart basins, concurrent with the rise of the adjacent topography and the correlative incision and entrenchment of major river courses, most notably of the Indus.

The combined inferences that the KF terminates west of Manasarovar Lake, that its total offset is only 66 km, and that it merges with the Gurla Mandatha detachment, consequently accounting for a comparable amount of slip on this low-angle feature [11], are not supported by our structural study of the area. There is no direct, linear connection between the KFZ and the Gurla Mandatha detachment since no significant right-lateral fault is seen in the field to cross the Amlang La ophiolite. One complex connection, through the active normal faults – not mapped by Murphy et al. [11] – which splay southwards from the KFZ at the NE corner of Manasarovar, might be envisaged (Fig. 6b,c). But such faults, which are deviated westwards by the northern boundary of the Gurla Mandatha anticlinorium (EW transfer zone) before veering along the eastern edge of the Pulan half graben, dip steeply and likely cut the detachment. In any event, the presence of identical geological units (Paleozoic of Raksas anticlinorium, ultramafics of Amlang La and Lalung Ri klippes) east and west of Manasarovar precludes more than a few kilometers of differential uplift across any of these faults. This, and the small length (≈ 20 km) of the transfer zone, make it unlikely that as much as 66 km of dextral motion have been absorbed along the west flank of Gurla Mandatha, as proposed by Murphy et al. [11]. Thus, most of the dextral motion along the KFZ west of the lakes likely continues east of them along the suture. The new structural and geometrical constraints shown in Fig. 6 in fact raise doubt on the significance of the 66 km maximum offset brought forward by Murphy et al. [11,13]. One consequence of the continuation of the KFZ eastwards along the suture is that the south Kailas 'counter' thrust cannot be used as a marker to define a piercing point [11,13] because it belongs to the transpressive fault zone and is roughly parallel to it (Fig. 6). Correlatively, the inferred age of this thrust (~ 13 Ma [13,25]) does not necessarily imply a post 13 Ma onset of dextral slip on the KFZ.

Our results also raise doubt on the offsets proposed by Searle and coworkers (e.g. [12,17]), which have increased by a factor of 2 in the last 10 years. Offset estimates of Baltoro-type granites initially inferred to be 85–90 km [17] were later

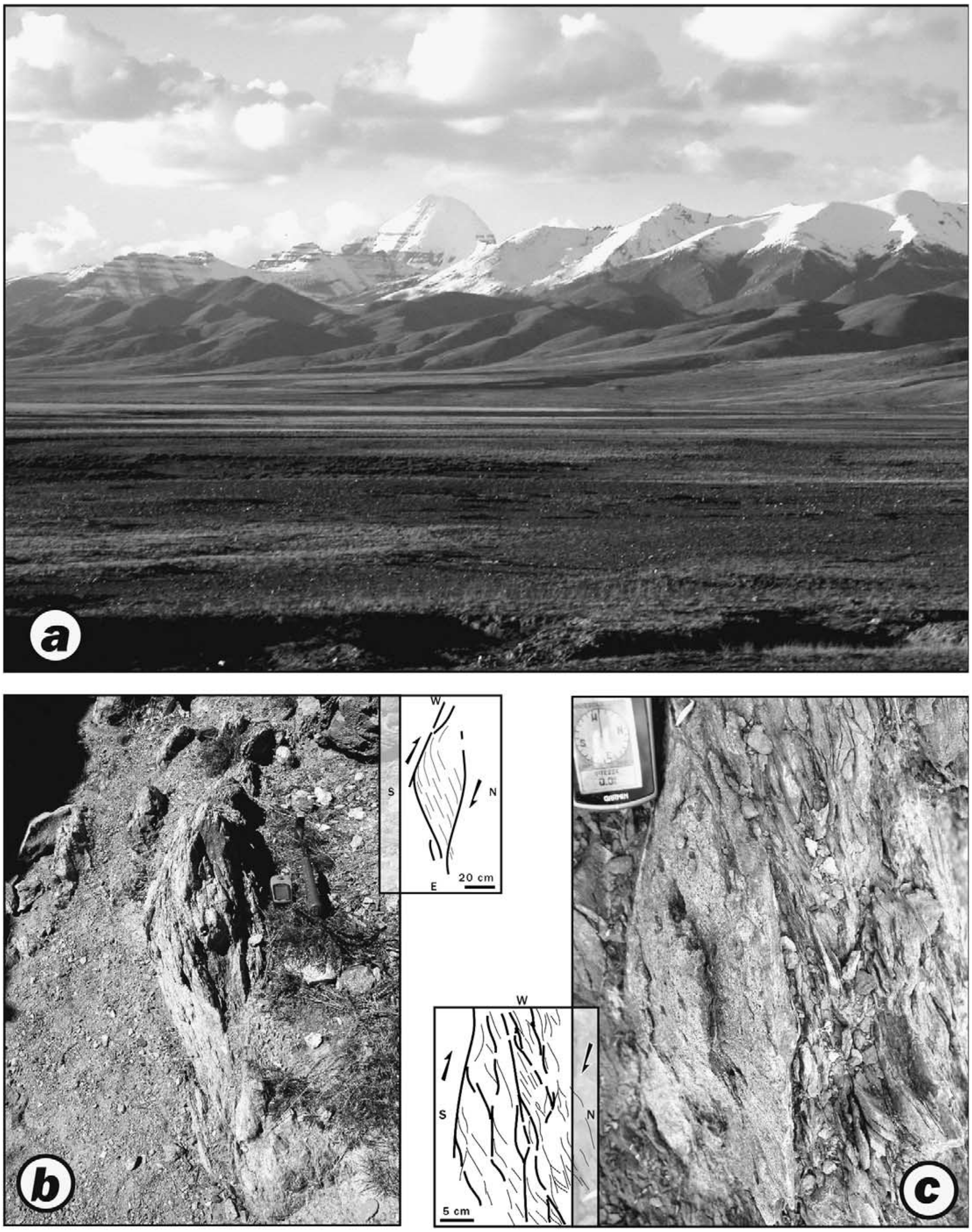

Fig. 7. a: View of Kailas-Ponri Range. Kailas is the rounded snowy mountain in the middle; note horizontal bedding in molasses beds below the summit. b,c: Typical characters of brittle-ductile deformation in southern Kailas flysch zone (vertical slivers and cleavage, sheared slivers and C/S shear planes); both images show structures on horizontal planes (oblique view towards west on b; view from above on c).

claimed to have been 120 km [12], following these authors' acknowledgment that total offsets of rocks could hardly be less than that of the Indus River course (> 115 km, [4,8,15]). Searle et al. [12] finally opted for a 150 km offset based on the correlation between the Baltoro and Tangtse leucogranites (Fig. 1). This value, however, can only represent a lower bound, as noted above, since the deformed Tangtse granite forms a sliver between two branches of the fault (see section in [12]) and is younger than the onset of dextral shear required by our new age data.

Part of the difficulties in estimating the total offset of the KFZ stems from the fact that the zone is complex (e.g. [20]) and splays into several branches (Fig. 1). Since in map view the ophiolite lenses SW of the Ladakh Range appear to be dextrally sheared boudins (Fig. 1), and since brittle dextral shear is clear along the Indus upstream from Leh (e.g. [28]), the 400-km-long N135°E-trending deflection between the suture zone east of Kailas and its counterpart west of Leh likely testifies to dextral offset of the suture [16]. Such motion would have taken place along a southern strand of the KFZ following the suture and branching off the northern strand near Menshi (Fig. 8). 400 km would represent an upper bound of the amount of dextral shear. To the northwest, such shear could have been absorbed in part by reactivation of the main mantle and main Karakorum thrusts (Figs. 1 and 8).

On the northern active branch of the fault, two of the clearest potential markers west of 80°E are Mesozoic ophiolite mélange belts older than the Zangbo suture: the Bangong and Shiquanhe suture zones (Figs. 1 and 8). The late Jurassic–early Cretaceous Bangong Nujiang suture of Tibet ([4,29], and references therein), is cleanly cut off south of 34°N by this branch. West of the fault, in the Pamir, the most likely continuation of this suture (Rushan-Pshart suture (e.g. [30])) is not exposed south of $\approx$37°N (Fig. 1). This implies a post $\approx$100 Ma offset greater than 400 km (Fig. 8, [4]). The Shiquanhe zone [4] is less continuous across Tibet, but includes peridotites, gabbros, cherts, together with a series of magmatic and volcaniclastic rocks (andesites, tuffs, greywackes) [4,31]. It is cut by the KF west of Shiquanhe at $\approx$32.5°N. The ultramafic and mafic rocks are associated with a Cretaceous sedimentary unit characterized by sandstones, conglomerates and Aptian orbitolinid and rudist-bearing limestones, overlain by red Tertiary sandstones [4,31]. This association led Matte et al. [4] to interpret this zone as a distinct late Cretaceous suture, although Kapp et al. [31] suggest that it might be part of the Bangong suture. In Ladakh and Pakistan, the Shyok suture, north of 34.5°N (Fig. 1), also comprises ultramafic, mafic and volcaniclastic rocks, associated with Aptian orbitolinid-rich limestones, overlain by red sandstones [32,33], which makes it a likely continuation of the Shiquanhe suture. Given the probable existence of a large ophiolitic boudin at $\approx$34.5°N, north of Tangtse, such a match would imply an offset of 280 ± 30 km or more if oblique thrusting occurred along the MKT (Fig. 8). Assuming that the Shiquanhe rocks belong to the Bangong suture [31], on the other hand, would imply that the Shyok suture has no counterpart in Tibet east of the KFZ [33], which we find unlikely.

We conclude that plausible Tertiary offsets on the southern and northern branches of the KFZ west of 81°E may be on an order of $\sim$300 km on either branch (Fig. 8). As these branches merge east of Menshi, this suggests that about 600 km of dextral shear might have taken place east of 81°E along the Zangbo suture and other adjacent faults, unless distributed clockwise block rotation, for which there is some evidence [20], occurred on a large scale between the Zangbo and the Karakorum-Jiali fault zone. Note that this value is 40% less than the maximum offset – 1000 km – loosely estimated by Peltzer and Tapponnier [14] from the separation between the tails of Gangdese and Ladakh granodiorite batholiths.

As with most major rivers crossing active faults, the 120 km offset of the Indus River course (Fig. 8) represents only a lower bound of finite motion along the northern branch of the KFZ [15]. Our thermochronological data near Zhaxigang suggest that the river might have become captive of the surrounding relief only after the onset of rapid uplift south of the fault at $\approx$12 Ma, a time at which it would have started to incise deeply across the Ladakh Range. This would imply dextral mo-

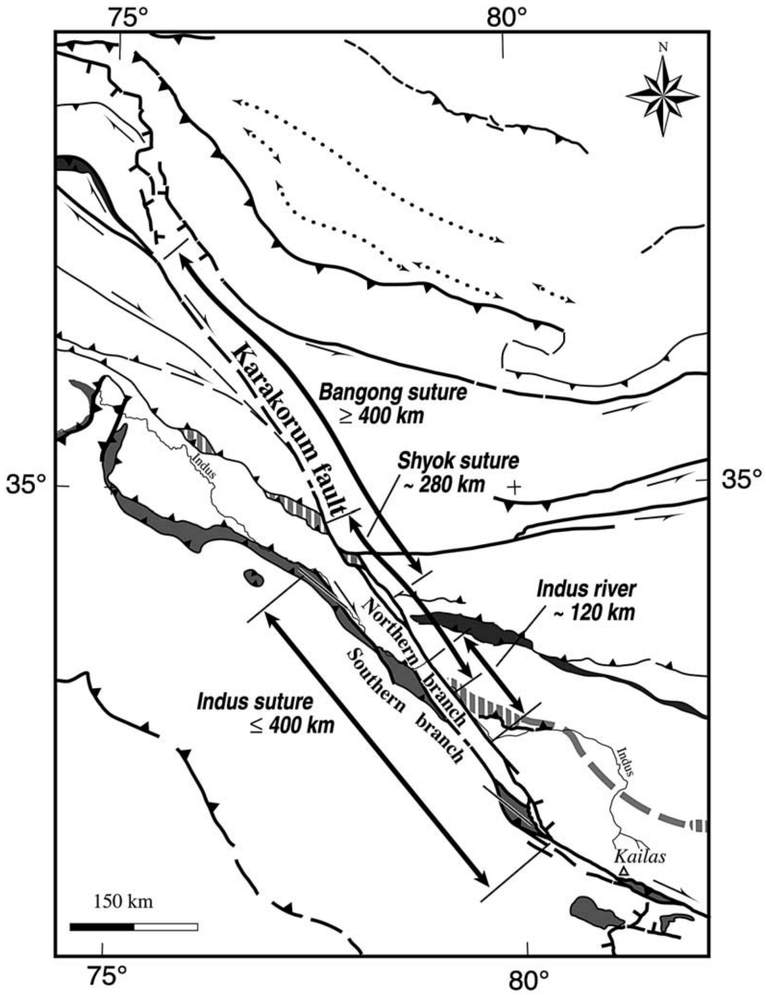

Fig. 8. Plausible offset values on the different branches of KFZ. See Fig. 1 for unit description, and text for discussion.

tion at a long-term average rate of 1 cm/yr, one third of the post-glacial rate of 3 cm/yr inferred by Qing [8], but more than twice the 4 mm/yr Holocene rate recently proposed by Brown et al. [10]. A comparable long-term value (1 ± 0.3 cm/yr) is obtained by assuming that 250–300 km of finite offset accrued in time spans of at least 23 and at most 32 Ma.

Though the values discussed here in the light of our new data remain first-order estimates with large uncertainties, it seems clear that minimum offsets < 100 km and average long-term rates < 1 cm/yr on the KF are not tenable. Likewise, a termination of the fault at Gurla Mandatha is most improbable. The KFZ and its probable continuation along the Yarlung Zangbo suture (Karakorum–Zangbo shear zone), likely contributed to absorb hundreds of kilometers of slip-partitioned convergence along the entire Karakorum–Himalayan arc [14,18–20] rather than acting as a shorter transfer fault restricted to the western part of the orogen.

Acknowledgements

We thank J.P. Brun and L. Ratschbacher for detailed and constructive reviews. Microprobe dating was performed at the CNRS-INSU national facility in Nancy under supervision of E. Deloule. Fieldwork was supported by the programs 'Intérieur de la Terre' (IT) and 'Dynamique et Evolution de la Terre Interne' (DYETI) of CNRS-INSU and by the Institute of Geology, Chinese academy of Geological Sciences, Beijing, China. A.C. Morillon is responsible for the quality of the figures. This is Institut de Physique du Globe de Paris contribution no. 1959.*[VC]*

References

[1] P.H. Leloup, R. Lacassin, P. Tapponnier, D. Zhong, X. Liu, L. Zhang, S. Ji, P.T. Trinh, The Ailao Shan-Red River shear zone (Yunnan, China), Tertiary transform boundary of Indochina, Tectonophysics 251 (1995) 3–84.

[2] P.H. Leloup, N. Arnaud, R. Lacassin, J.R. Kienast, T.M. Harrison, P.T. Trinh, A. Replumaz, P. Tapponnier, New constraints on the structure, thermochronology and timing of the Ailao Shan–Red River shear zone, J. Geophys. Res. 106 (2001) 6657–6671.

[3] G. Wittlinger, P. Tapponnier, G. Poupinet, M. Jiang, D. Shi, G. Herquel, F. Masson, Tomographic evidence for localized shear along the Altyn Tagh fault, Science 282 (1998) 74–76.

[4] P. Matte, P. Tapponnier, N. Arnaud, L. Bourjot, J.P. Avouac, P. Vidal, Q. Liu, Y. Pan, Y. Wang, Tectonics of Western Tibet, between the Tarim and the Indus, Earth Planet. Sci. Lett. 142 (1996) 311–330.

[5] B.D. Ritts, U. Biffi, Magnitude of post-middle Jurassic (Bajocian) displacement on the central Altyn Tagh fault system, Northwest China, Geol. Soc. Am. Bull. 112 (2000) 61–74.

[6] P. Tapponnier, Z. Xu, F. Roger, B. Meyer, N. Arnaud, G. Wittlinger, J. Yang, Oblique stepwise rise and growth of the Tibet plateau, Science 294 (2001) 1671–1677.

[7] A. Yin, P.E. Rumelhart, R. Butler, E. Cowgill, T.M. Harrison, D.A. Foster, R.V. Ingersoll, Q. Zhang, X. Zhou, X. Wang, A. Hanson, A. Raza, Tectonic history of the Altyn Tagh fault system in northern Tibet inferred from Cenozoic sedimentation, Geol. Soc. Am. Bull. 114 (2002) 1257–1295.

[8] Qing, L., Paléoclimats et contraintes chronologiques sur les mouvements récents dans l'ouest du Tibet: failles du Karakorum et de Longmu Co–Gozha Co, lacs en pull-apart de Longmu Co et de Sumxi Co., PhD, Université Paris 7, 1993.

[9] J.-P. Avouac, P. Tapponnier, Kinematic model of active deformation in central Asia, Geophys. Res. Lett. 20 (1993) 895–898.

[10] E.T. Brown, R. Bendick, D.L. Bourlès, V. Gaur, P. Molnar, G.M. Raisbeck, F. Yiou, Slip rates of the Karakorum fault, Ladakh, India, determined using cosmic ray exposure dating of debris flows and moraines, J. Geophys. Res. 107 (2002) ESE7-1–ESE7-13.

[11] M.A. Murphy, A. Yin, P. Kapp, T.M. Harrison, C.E. Manning, F.J. Ryerson, L. Ding, J. Guo, Structural evolution of the Gurla Mandatha detachment system, southwest Tibet: implications for the eastward extent of the Karakoram fault system, Geol. Soc. Am. Bull. 114 (2002) 428–447.

[12] M.P. Searle, R.F. Weinberg, W.J. Dunlap, Transpressional tectonics along the Karakoram fault zone, northern Ladakh: constraints on Tibetan extrusion, in: R.E. Holdsworth, R.E. Strachan, J.F. Dewey (Eds.), Continental Transpressional and Transtensional Tectonics, Geological Society Special Publications 135, Geological Society, London, 1998, pp. 307–326.

[13] M.A. Murphy, Y. An, P. Kapp, T.M. Harrison, L. Ding, J. Guo, Southward propagation of the Karakoram fault system, southwest Tibet Timing and magnitude of slip, Geology 28 (2000) 451–454.

[14] G. Peltzer, P. Tapponnier, Formation and evolution of strike-slip faults, rifts, and basins during India–Asia collision: an experimental approach, J. Geophys. Res. 93 (1988) 15085–15117.

[15] Y. Gaudemer, P. Tapponnier, D.L. Turcotte, River offsets across active strike-slip faults, Ann. Tecton. 3 (1989) 55–76.

[16] L. Ratschbacher, W. Frisch, U. Herrman, M. Strecker, Distributed deformation in southern and western Tibet during and after the India–Asia collision: An experimental approach, J. Geophys. Res. 99 (1994) 19917–19945.

[17] M.P. Searle, Geological evidence against large-scale pre-Holocene offsets along the Karakoram Fault: implications for the limited extrusion of the Tibetan plateau, Tectonics 15 (1996) 171–186.

[18] R. McCaffrey, J. Nabelek, Role of oblique convergence in the active deformation of the Himalayas and southern Tibet plateau, Geology 26 (1998) 691–694.

[19] P. Tapponnier, G. Peltzer, R. Armijo, On the mechanics of the collision between India and Asia, in: M.P. Coward, A.C. Ries (Eds.), Collision Tectonics, Geological Society Special Publication 19, Geological Society, London, 1986, pp. 115–157.

[20] R. Armijo, P. Tapponnier, H. Tonglin, Late Cenozoic right-lateral strike-slip faulting in southern Tibet, J. Geophys. Res. 94 (1989) 2787–2838.

[21] O.M. lovera, F.M. Richter, T.M. Harrison, The $^{40}Ar/^{39}Ar$ thermochronometry for slowly cooled samples having a distribution of diffusion domain sizes, J. Geophys. Res. 94 (1989) 17917–17935.

[22] N. Arnaud, Apports de la thermochronologie $^{40}Ar/^{39}Ar$ sur feldspath potassique à la connaissance de la tectonique cénozoïque d'Asie, PhD thesis, Université Clermont-Ferrand, 1992.

[23] A. Gansser, Geology of the Himalayas, Wiley, London, 1964, 289 pp.

[24] R. Armijo, P. Tapponnier, J.L. Mercier, H. Tonglin, Qua-

ternary extension in southern Tibet: field observations and tectonic implications, J. Geophys. Res. 91 (1986) 13803–13872.

[25] A. Yin, T.M. Harrison, M.A. Murphy, M. Grove, S. Nie, Tertiary deformation history of southeastern and southwestern Tibet during the Indo-Asian collision, Geol. Soc. Am. Bull. 111 (1999) 1644–1664.

[26] U. Schärer, L.-S. Zhang, P. Tapponnier, Duration of strike-slip movements in large shear zones: The Red River belt, China, Earth Planet. Sci. Lett. 126 (1994) 379–397.

[27] R.F. Weinberg, M.P. Searle, The Pangong injection complex, Indian Karakoram: a case of pervasive granite flow through hot viscous crust, J. Geol. Soc. 155 (1998) 883–891.

[28] A. Steck, L. Spring, J.C. Vannay, H. Masson, E. Stutz, H. Bucher, R. Marchant, J.C. Tièche, Geological transect across the Northwestern Himalaya in eastern Ladakh and Lahul (a model for the continental collision of India and Asia), Eclog. Geol. Helv. 86 (1993) 219–263.

[29] C. Chang, N. Chen, M.P. Coward, W. Deng, J. Dewey, A. Gansser, N.B.W. Harris, C. Jin, W.S.F. Kidd, M.R. Leeder, H. Li, J. Lin, C. Liu, M. Houjun, P. Molnar, Y. Pan, Y. Pan, J.A. Pearce, R.M. Shackleton, A.B. Smith, Y. Sun, M. Ward, D.R. Watts, J. Xu, R. Xu, J. Yin, Y. Zhang, Preliminary conclusions of the Royal Society and Academia Sinica 1985 geotraverse of Tibet, Nature 323 (1986) 501–507.

[30] M.N. Ducea, V. Lutkov, V.T. Minaev, B. Hacker, L. Ratschbacher, P. Luffi, M. Schwab, G.E. Gehrels, M. McWilliams, J. Vervoort, J. Metcalf, Building the Pamirs, the view from the underside, Geology 31 (2003) 849–852.

[31] P. Kapp, M.A. Murphy, A. Yin, T.M. Harrison, D. Lin, G. Jinghu, Mesozoic and Cenozoic tectonic evolution of the Shiquanhe area of western Tibet, Tectonics 22 (2003) 3.1–3.21.

[32] W.J. Dunlap, R. Wysoczanski, Thermal evidence for early Cretaceous metamorphism in the Shyok suture zone and age of the Khardung volcanis rocks, Ladakh, India, J. Asian Earth Sci. 20 (2002) 481–490.

[33] Y. Rolland, A. Pêcher, C. Picard, Middle Cretaceous back-arc formation and arc evolution along the Asian margin: the Shyok suture zone in northern Ladakh (NW Himalaya), Tectonophysics 325 (2000) 145–173.

[34] Geology Publishing House, Geological Map of Qinhai-Xizang Plateau and Adjacent Areas, Geology Publishing House, Beijing, 1998.